Classical and Neo-Classical Cruise-Dash Optimization

K. D. Bilimoria,* E. M. Cliff,† and H. J. Kelley‡
Virginia Polytechnic Institute and State University, Blacksburg, Virginia

Cruise-dash flight performance is examined in the context of singular perturbations and is shown to be the "outer" solution of a dynamic flight-path optimization problem. It is found that certain velocity regions are nonoptimal for cruise-dash and that optimal cruise-dash sometimes requires time-shared operation between two altitude-airspeed points. This is illustrated computationally by example.

Introduction

THIS paper investigates the problem of determining an atmospheric flight path between given endpoints that minimizes a linear combination of time and fuel. In the following section the trajectory-shaping problem will be formulated for a point-mass model and it will be demonstrated that rectilinear cruise is an "outer" solution when Newtonian dynamics are "fast." A subsequent section will discuss the resulting classical cruise-dash problem. In particular, it will be shown that nonconvexity in the fuel-flow vs airspeed graph has important consequences in optimum-cruise problems with time restrictions. Some computations will then be presented illustrating the sometime occurrence of time-shared operation between two altitude-airspeed combinations for optimal cruise-dash.

Problem Formulation

While this paper is primarily concerned with classical cruise-dash analysis, it is appropriate to consider the connection between cruise-dash performance and the more general problem of flight-path optimization. For this purpose one begins with the point-mass model, albeit in a somewhat special form:

$$\epsilon_2 \dot{h} = V \sin\gamma \tag{1}$$

$$\epsilon_2 \dot{\gamma} = (g/V)\left(\frac{(L+\epsilon_3 T\,\sin\alpha)\cos\mu}{(W_0-\epsilon_3 W_F)} - \cos\gamma\right) \tag{2}$$

$$\epsilon_1 \dot{E} = \frac{(T-D)V+\epsilon_3 T\,V(\cos\alpha-1)}{(W_0-\epsilon_3 W_F)} \tag{3}$$

$$\epsilon_1 \dot{\chi} = \frac{g\,L\,\sin\mu}{(W_0-\epsilon_3 W_F)\,V\cos\gamma} \tag{4}$$

$$\dot{x} = V\cos\gamma\cos\chi \tag{5}$$

$$\dot{y} = V\cos\gamma\sin\chi \tag{6}$$

$$\dot{W}_F = Q \tag{7}$$

These are the equations for three-dimensional aircraft flight with zero sideforce over a flat, nonrotating Earth. In these equations h is the altitude, γ the path angle, E the energy per unit weight, χ the velocity-heading angle, x and y the northerly and easterly position components, and W_F the weight of fuel consumed. The symbol V is to be regarded as a convenient shorthand for the quantity $[2g(E-h)]^{1/2}$, where g is the acceleration due to gravity. L and D denote the usual aerodynamic force components, lift and drag, respectively, and W_0 is the initial weight of the aircraft. T is the thrust and Q the fuel-flow rate; both are functions of Mach number and altitude, and depend on a throttle parameter η. The angle α is angle of attack, while μ is the bank angle.

The parameters ϵ_1 and ϵ_2 are introduced as in Ref. 1 to motivate an order reduction, while ϵ_3 is convenient for imbedding certain complicating effects. In particular, with $\epsilon_3 = 0$, the model has constant aircraft weight and thrust along the path. Complications such as nonstandard atmosphere or winds aloft might be treated in the same manner in terms of ordinary perturbations.

In addition to the dynamical equations, the system is subjected to certain inequality constraints involving state and control variables:

$\beta_1 = (h-h_T) \geq 0$ (terrain limit)

$\beta_2 = (\bar{q}-g\rho(E-h)) \geq 0$ (dynamic pressure limit)

$\beta_3 = (\bar{M}-M) \geq 0$ (Mach limit)

$\beta_4 = (\bar{n}W - C_L qS) \geq 0$ (normal load-factor limit)

$\beta_5 = (\bar{C}_L(M) - C_L) \geq 0$ (aerodynamic limit)

In these constraints h_T is the minimum allowable altitude, while $\bar{q}$, $\bar{M}$, $\bar{n}$, and $\bar{C}_L$ are maximum allowable values of dynamic pressure, Mach number, normal load factor, and lift coefficient, respectively. The last is a specified function of Mach number. The path-optimization problem to be considered is as follows: Choose the controls C_L (or α), μ, and η to transfer the system from a given initial point (h_0, γ_0, E_0, χ_0, x_0, y_0) to a given final point (h_f, γ_f, E_f, χ_f, x_f, y_f) while minimizing a Mayer-type cost function

$$C = \mu_1 t_f + \mu_2 W_F(t_f)$$

In this cost function, t_f is the unspecified final time and $W_F(t_f)$ the weight of fuel consumed at $t = t_f$. The parameters μ_1 and μ_2 are specified to represent a tradeoff between time and fuel. In particular, with $\mu_1 = 0$ and $\mu_2 > 0$ the problem is to minimize fuel, while with $\mu_1 > 0$ and $\mu_2 = 0$ the problem is

Received Feb. 2, 1984; presented as Paper 84-2125 at the AIAA Atmospheric Flight Mechanics Conference, Seattle, Wash., Aug. 21-23, 1984; revision submitted Feb. 27, 1985.

*Graduate Research Assistant, Department of Aerospace and Ocean Engineering. Student Member AIAA.

†Professor, Department of Aerospace and Ocean Engineering. Member AIAA.

‡Professor, Department of Aerospace and Ocean Engineering. Fellow AIAA.

to minimize time. Note that the range is specified for this problem.

To "solve" this optimization problem one proceeds to form the variational Hamiltonian and, with the prejudice of foresight, defines

$$H = H_1 + H_2 \tag{8}$$

$$H_1 = \lambda_x V \cos\gamma \cos\chi + \lambda_y V \cos\gamma \sin\chi + \lambda_{W_F} Q \tag{9}$$

$$H_2 = \lambda_h f_h + \lambda_\gamma f_\gamma + \lambda_E f_E + \lambda_\chi f_\chi \tag{10}$$

The terms λ_i denote Lagrange multipliers, and the terms f_i in H_2 are a shorthand for the right members of the respective dynamical equations.

One might now apply the minimum principle[2,3] to this problem, deducing the state-Euler equations with appropriate boundary conditions. The results would be a two-point boundary-value problem involving a fourteenth-order system of differential equations. While this may be solvable with modern computer software, its usefulness in onboard intercept guidance might be questioned in the current state-of-the-art.

The interpolation parameters ϵ_1 and ϵ_2 separate the aircraft equations of motion into three time scales involving "fast," "intermediate," and "slow" state variables. The approach here, as in Ref. 1, is to begin by considering the problem for the reduced system with $\epsilon_1 = \epsilon_2 = \epsilon_3 = 0$. In this case the dynamical system involves only three state variables x, y, W_F (note that time is state-like since it appears in the performance index) and seven control variables h, γ, E, χ, μ, C_L, and η. With $\epsilon_1 = \epsilon_2 = 0$ the first four system equations become constraints from which one deduces (for $\epsilon_3 = 0$) that

$$\mu = 0 \tag{11}$$

$$\gamma = 0 \tag{12}$$

$$L = W_0 \tag{13}$$

$$T = D \tag{14}$$

Lift equals weight can be "solved" for C_L given E and h, while thrust equals drag can then be "solved" for η. With these explicit conditions the part of the Hamiltonian labeled H_2 is guaranteed to be zero. Hence, the min-H operation amounts to selecting η, E, h, and χ to minimize H_1, subject to the inequality constraints, $\beta_i \geq 0$. Observe that, with $\epsilon_3 = 0$, none of the state variables x, y, or W_F appear on the right-hand side of a state equation so that the corresponding costates λ_x, λ_y, and λ_{W_F} are constant in time.

Proceeding with the min-H operation one expresses the unknown costates λ_x and λ_y in polar form as

$$\lambda_x = A \cos\Lambda \tag{15}$$

$$\lambda_Y = A \sin\Lambda \tag{16}$$

where $A \geq 0$; and rewrites the Hamiltonian as

$$H_1 = V A \cos(\chi - \Lambda) + \lambda_{W_F} Q \tag{17}$$

It is clear that the appropriate choice is $\Lambda = (\chi - \pi)$, where χ is selected so that the rectilinear path goes through the specified points (x_0, y_0) and (x_f, y_f).

$$\chi = \tan^{-1}[(y_f - y_0)/(x_f - x_0)] \tag{18}$$

The terminal transversality condition requires[2,3] that

$$H_1(t_f) = -\mu_1 \tag{19}$$

$$\lambda_{W_F}(t_f) = \mu_2 \tag{20}$$

from which one finds

$$A = [\mu_1 + \mu_2 Q(t_f)]/V(t_f) \tag{21}$$

so that

$$H_1 = -\{[\mu_1 + \mu_2 Q(t_f)]/V(t_f)\} V + \mu_2 Q \tag{22}$$

One now defines constants λ_F (fuel) and λ_R (range) by

$$\lambda_F = \mu_2 \tag{23}$$

$$\lambda_R = [\mu_1 + \mu_2 Q(t_f)]/V(t_f) \tag{24}$$

and observes that the min-H operations can be interpreted as seeking a point (given by E, h, and η) that minimizes the quantity

$$J = \lambda_F Q - \lambda_R V \tag{25}$$

subject to level-flight equilibrium constraints and the inequality constraints $\beta_i \geq 0$. This is a classical cruise-dash problem and will be examined in some detail. The approach taken here will be to solve this problem for specified λ_F and λ_R and compute the corresponding μ_1 and μ_2 from

$$\mu_1 = \lambda_R V - \lambda_F Q = -J_{\min} \tag{26}$$

$$\mu_2 = \lambda_F \tag{27}$$

Cruise-Dash Analysis

The problem considered here is that of finding a point on or within the flight envelope, characterized by a speed V, an altitude h, and a throttle setting η, that minimizes the quantity

$$J = \lambda_F Q(\eta, h, V) - \lambda_R V$$

subject to the level-flight equilibrium constraints and the inequality constraints $\beta_i \geq 0$.

The parameters λ_F and λ_R are specified constants and their relation to the parameters μ_1 and μ_2 in the dynamic performance index has been described above. Recapitulating some of the previous discussion, one notes that for a given pair (h, V) the equation $L = W_0$ is to be "solved" for C_L. One then evaluates the corresponding drag $D(h, V, C_L)$ and then solves for the throttle setting η such that $T(\eta, h, V)$ equals the determined value for drag. If the throttle setting that emerges is not admissible (e.g., drag greater than maximum available thrust), then one might set J equal to positive infinity and, in this way, interpret J to be a function of h and V.

To proceed with the analysis, note that the second term in the sum for J depends only on V and since

$$\min_{h,V} J(V,h) = \min_{V} [\min_{h} J(V,h)]$$

one is led to consider minimizing the fuel flow over altitude for fixed V. Accordingly, one defines

$$Q^*(V) = \min_h [Q(\eta, h, V)] \tag{28}$$

and

$$J^*(V) = \lambda_F Q^*(V) - \lambda_R V \tag{29}$$

so that the cruise-dash problem can be restated as seeking the velocity V that minimizes the combination $(\lambda_F Q^*(V)$

$-\lambda_R V$). A method of characterizing solutions to this problem can be easily explained in geometrical terms set in the (Q,V) plane. For fixed (non-negative) values of λ_F and λ_R, lines of constant $(\lambda_F Q - \lambda_R V)$ are as shown in Fig. 1 with values increasing as one moves upward (increasing Q) or to the left (decreasing V). If one superposes a graph of $Q^*(V)$, then it is seen that an optimal (V,Q) is a point of contact of the $Q^*(V)$ graph and that member of the constant $(\lambda_F Q - \lambda_R V)$ family that separates the part of the plane containing the graph from the part of the plane containing no points on the graph. In optimization theory[4] this is called a *supporting hyperplane*—in this case it is a line. From Fig. 1 it can be seen that if $Q^*(V)$ is smooth, then

$$\left(\frac{dQ^*}{dV}\right)_{V_0} = \frac{\lambda_R}{\lambda_F} \tag{30}$$

The *necessity* of this tangency condition, under the smoothness assumption on $Q^*(V)$, can be established from the usual requirement that the first derivative of $J^*(V)$ must vanish at a minimizing V.

Computations and Results

A computational study of cruise-dash optimization was carried out using data for a twin-engined high-performance military aircraft. The atmospheric, aerodynamic, and propulsive modeling is presented in Appendix A. Only the aerodynamic limit [defined by $\bar{C}_L(M)$] was considered in this study, and the terrain limit was sea level.

The $Q^*(V)$ graphs obtained from a one-dimensional minimization over altitude are presented in Figs. 2 and 3. Details of the numerical procedures used to calculate $Q^*(V)$ are included in Appendix B. Figures 4 and 5 include the graphs of optimal altitude and throttle setting that emerge from the min-Q operation over altitude. As described in Appendix A, $\eta = 0$ corresponds to zero thrust, $\eta = 1$ to military thrust, and $\eta = 2$ implies full afterburning thrust. The most interesting features of the $Q^*(V)$ graph are its regions of nonconvexity. These imply that the tangency condition [Eq. (30)] is not sufficient for optimality. In other words, a tangent line need not be a "supporting" line (see Fig. 6 which shows three candidates labeled X, Y, and Z).

We now consider the problem of characterizing the minimizing V in terms of the parameter λ_{FR} $(=\lambda_F/\lambda_R)$. Cruise-dash points are computed for values of λ_{FR} ranging from 0 to 10^6 ft/lb, thus covering the entire spectrum from the high-speed point to the minimum-fuel-flow point, respectively (Fig. 7). It is observed that the locus of optimal operating points has several discontinuities, and that the jumps in velocities are closely related to the nonconvexities in the $Q^*(V)$ graph. As an illustration, consider the behavior of the cruise-dash locus, starting at the fixed-range minimum-fuel point ($h = 46{,}510$ ft, $V = 775$ fps) with $\lambda_{FR} = 1000$ ft/lb. As λ_{FR} decreases, the emphasis on velocity

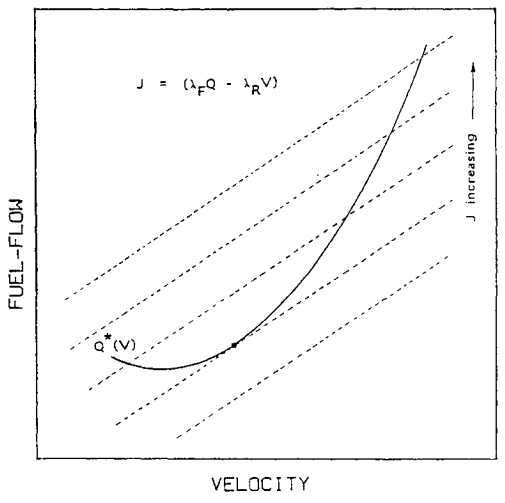

Fig. 1 Lines of constant $J = (\lambda_F Q - \lambda_R V)$ and $Q^*(V)$.

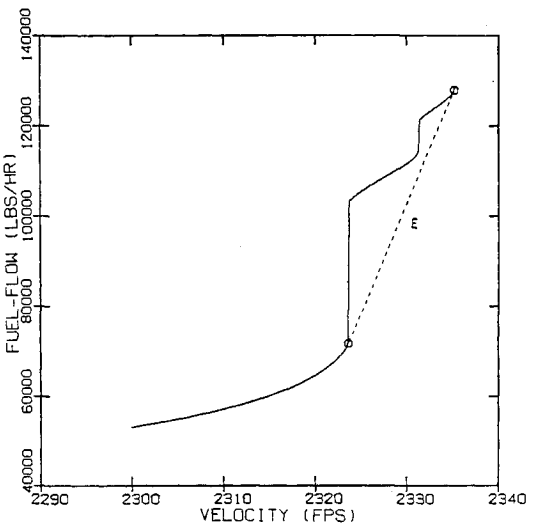

Fig. 3 Miminum fuel flow $Q^*(V)$ velocity (high-speed region).

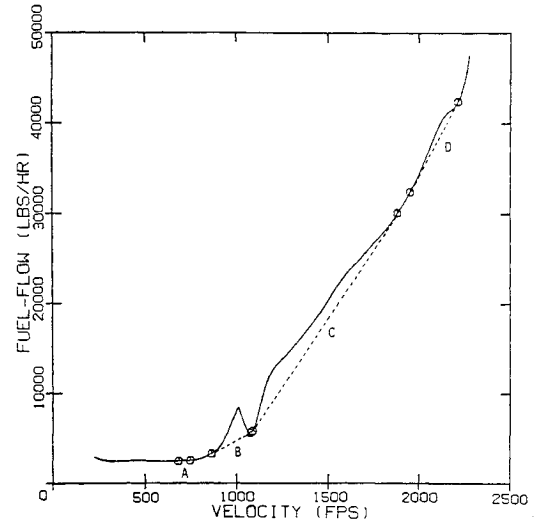

Fig. 2 Minimum fuel flow $Q^*(V)$ vs velocity.

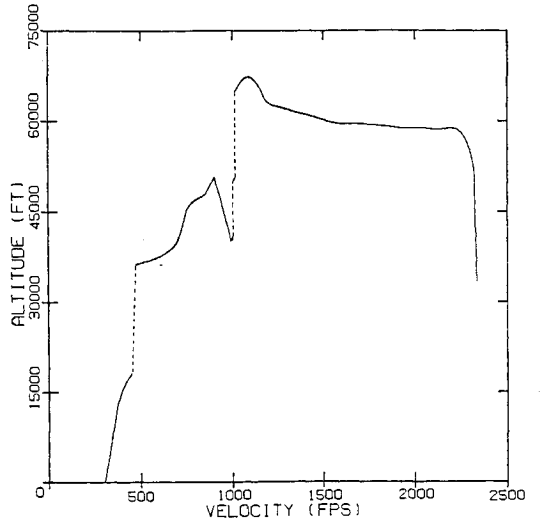

Fig. 4 Fuel-minimizing altitude h_0 vs velocity.

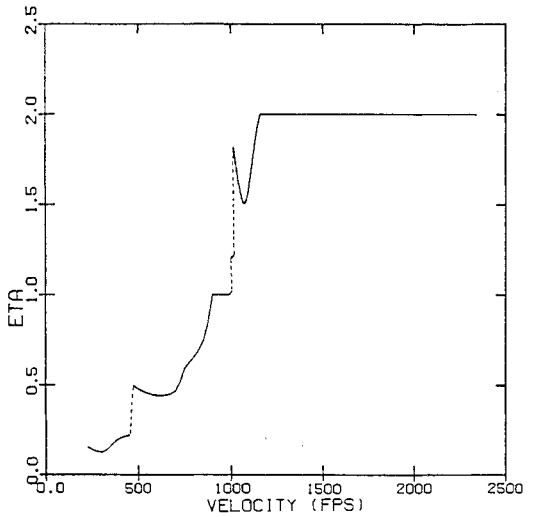

Fig. 5 Fuel-minimizing throttle setting η_0 vs velocity.

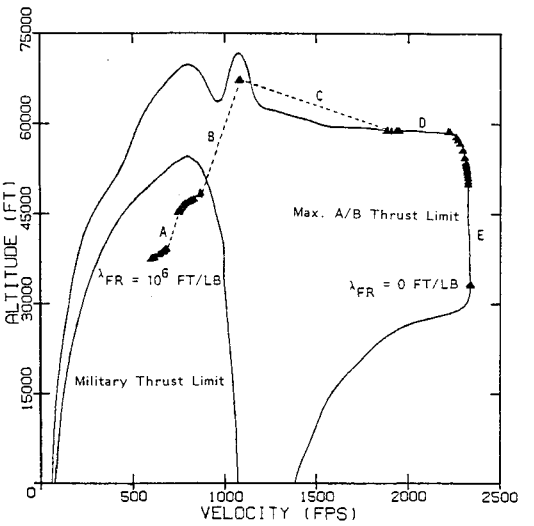

Fig. 7 Cruise dash points and flight envelopes in the (h, V) plane.

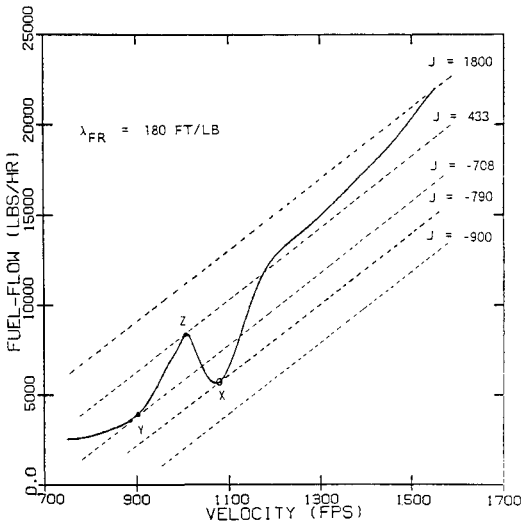

Fig. 6 Candidate minima of $J=(\lambda_F Q-\lambda_R V)$.

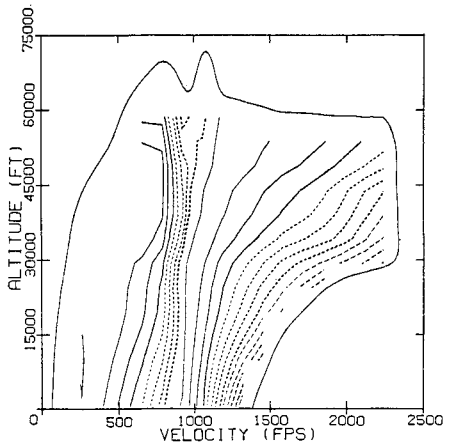

Fig. 8 Constant fuel-flow contours for level unaccelerated flight.

(range) in the performance index increases while the importance of fuel flow decreases. Figure 8 presents the flight envelope along with loci of constant fuel flow for unaccelerated level flight. From these contours one might expect that as λ_{FR} decreases the cruise-dash altitude and velocity both would increase. The cruise-dash locus does in fact follow this trend, with velocity and altitude both increasing until λ_{FR} reaches 319.36 ft/lb. At this value, the cruise-dash point abruptly jumps from ($h=48{,}535$ ft, $V=864$ fps) to ($h=67{,}179$ ft, $V=1075$ fps). The explanation for this behavior can be found in Fig. 6 which shows a region of the $Q^*(V)$ curve. It can be seen that $Q^*(V)$ exhibits nonconvex behavior in the range 864 fps$<V<$1075 fps, so that a supporting line will not touch the curve for any velocity in this region. Therefore there can be no cruise-dash points in this velocity range, thus explaining the gap in the cruise-dash locus.

The $Q^*(V)$ graph (Figs. 2 and 3) has several regions of nonconvexity and thus the locus of optimal operating points characterized by λ_{FR} has several gaps (see Fig. 7). Note that there is a one-to-one correspondence between nonconvexities in the (Q, V) plane and discontinuities of the cruise-dash locus in the (h, V) plane, both labeled A-E in Figs. 2, 3, and 7.

There is another interesting consequence of the nonconvexity of the function $Q^*(V)$. Consider the question of minimum-fuel transport for the kinematic model ($\epsilon_1=\epsilon_2=0$) with specified *average* speed. The classical cruise exercise is to seek the altitude h_0 and throttle setting η_0 that minimizes $Q(\eta, h, V_0)$ with V_0 specified. Note that this will produce fuel flow $Q^*(V_0)$. If V_0 is in a region of nonconvexity of $Q^*(V)$ then one could do better by flying at speeds V_1 and V_2 (see Fig. 9) with time at each apportioned to average V_0. Figure 10 shows the fuel savings as a function of velocity. The cruise-dash model features instantaneous changes in energy and altitude, hence the transition from one operating point to the other is achieved with zero fuel consumption.

One could even achieve *constant average* speed V_0 by "chattering"[5] between V_1 and V_2. [Note that for the reduced model the graph of the function $Q^*(V)$ traces out the boundary of the hodograph figure.] The simplest and most frequently occurring type of time-shared operation would seem to feature a single transition between two (h, V) points. The order of the sequence is ambiguous in zeroth-order asymptotic approximation. More complex time sharing (possible "chattering") may correspond to oscillatory cruise dash in optimal flight with a point-mass vehicle model.[6-8]

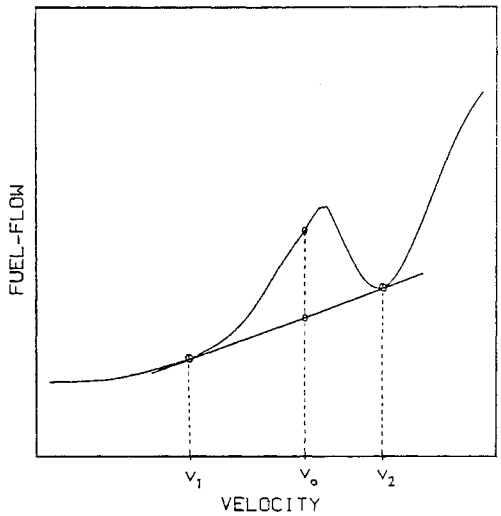

Fig. 9 A nonconvex region of $Q^*(V)$ vs velocity.

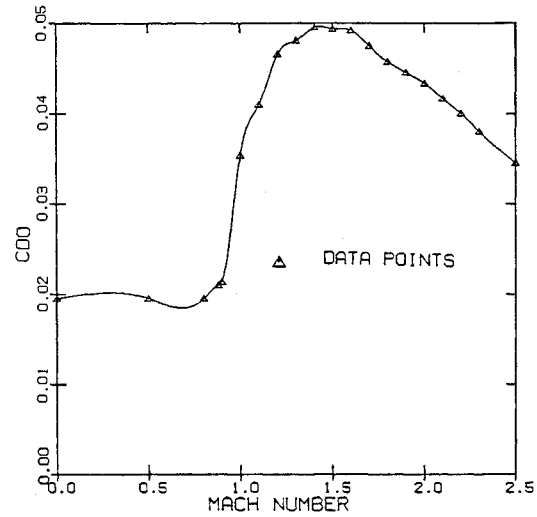

Fig. A1 Zero-lift drag coefficient C_{D0} vs Mach number.

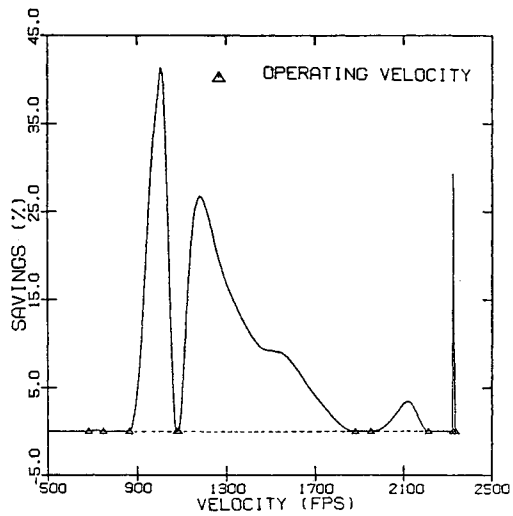

Fig. 10 Fuel savings for time-shared operation.

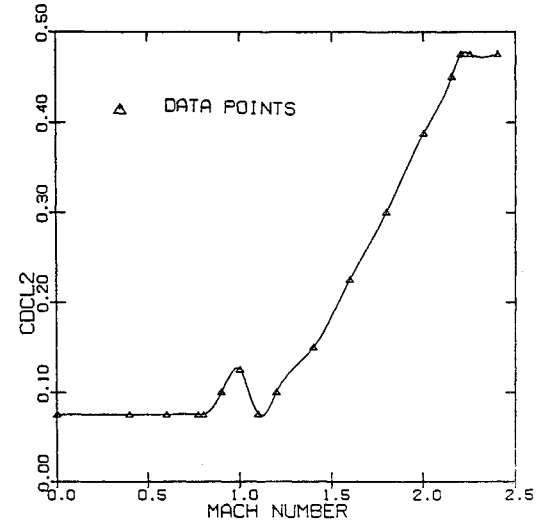

Fig. A2 Induced drag coefficient $C_{D_{CL2}}$ vs Mach number.

Conclusions

The classical problem of selecting an altitude, velocity, and throttle setting to minimize a linear combination of fuel flow and (negative) range rate has been considered as an "outer" solution of a dynamic path-optimization problem, when Newtonian dynamics are modeled as "fast." This classical cruise-dash problem has a family of solutions where each member depends on the relative emphasis placed on time and fuel. Computations performed for a particular high-performance aircraft show that the locus of optimal operating points has several breaks, each corresponding to a nonconvexity in the $Q^*(V)$ curve. Consequently, certain velocity regions are nonoptimal for cruise-dash operation.

If a time constraint forces operation at an average velocity in such a region, time-shared operation is more fuel efficient than classical (steady-state) cruise. This behavior may be interpreted as a simple sequence of operation at two (h, V) points or, possibly, as "chattering," corresponding to oscillatory cruise dash in point-mass modeling.

Appendix A: Modeling

Atmosphere

Air density (slugs/ft^3) and sonic velocity (ft/s) are supplied in tabular form as functions of altitude (ft). The sonic velocity and the natural logarithm of the air density are interpolated as cubic-spline functions of altitude.[9] The acceleration due to gravity (ft/s^2) is a specified constant.

Aerodynamics

The aircraft drag coefficient C_D is computed as a parabolic function of lift coefficient C_L with polar parameters C_{D0} and C_{DCL2}, both of which are supplied in tabular form as functions of Mach number. The maximum lift coefficient $\bar{C}_L$ is also specified as a function of Mach number. C_{D0}, C_{DCL2}, and $\bar{C}_L$ are interpolated as cubic-spline functions of Mach number. This is shown for C_{D0} and C_{DCL2} in Figs. A1 and A2. The aircraft weight (lb) and aerodynamic reference area (ft^2) are specified constants.

Propulsion

Two sets of thrust (lb) and fuel-flow (lb/hr) tables are available as functions of Mach number and altitude (ft). One set corresponds to military (maximum nonafterburning) operation, and the other represents operation with full afterburner. The afterburning thrust and fuel-flow data are presented in Figs. A3 and A4. Interpolation of these tables between (h,M) points is done by using cubic-spline lattices.[9]

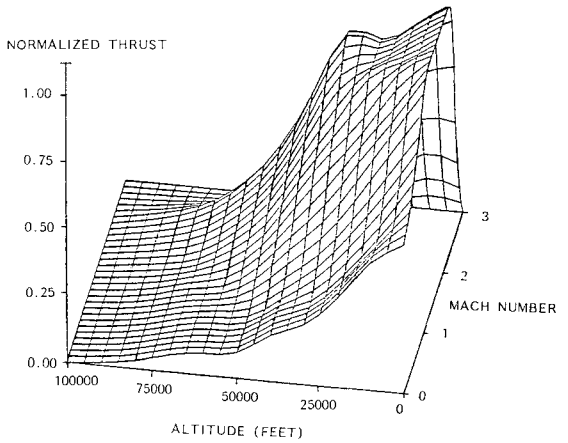

Fig. A3 Maximum afterburning thrust vs Mach number and altitude.

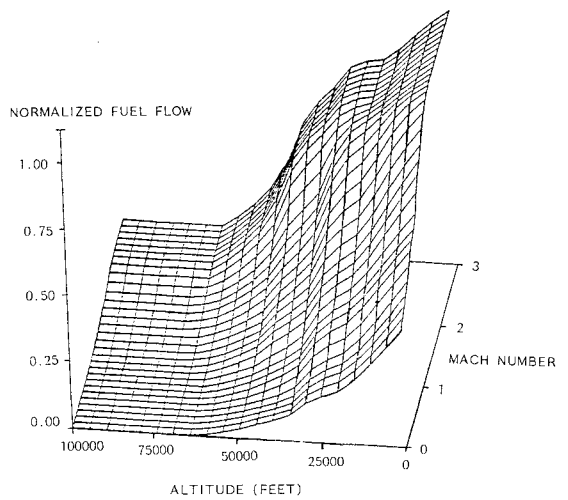

Fig. A4 Maximum afterburning fuel flow vs Mach number and altitude.

Interpolation between military and afterburning is linear as is partial-throttle military. One introduces a throttle parameter η such that operation at military power corresponds to throttle setting $\eta = 1$, and throttle setting $\eta = 2$ gives full afterburning operation. $\eta = 0$ is a zero-thrust setting. Thrust and fuel-flow values (for a given altitude and Mach number) are known only for three throttle settings, $\eta = 0$, 1, and 2. A linear variation in throttle is assumed between $\eta = 0$, 1 and $\eta = 1$, 2, hence given a value of thrust, the throttle setting can be computed by linear interpolation. Note that this is not truly an assumption; indeed it serves only to define the throttle parameter η. However, one now assumes that fuel flow also varies in a sectionally linear way with η. Thus, the specific fuel consumption is independent of throttle for idle-to-military settings and the incremental specific fuel consumption in afterburning operation is also independent of throttle. Given that one only has propulsive data at three throttle settings, a sectionally linear model is reasonable. However, the results obtained may well be influenced by this type of modeling. Finally, note that the "data" at $\eta = 0$ is taken as $T = Q = 0$.

Appendix B: Computation of $Q^*(V)$

By definition,

$$Q^*(V) = \min_h [Q(\eta, h, V)]$$

Given a (h, V) pair, the thrust T and throttle setting η can be computed by making use of $L = W_0$ and $T = D$ as described in the section on Cruise-Dash Analysis. Since the values of fuel flow are known for three throttle settings ($\eta = 0,1,2$), one can evaluate $Q(\eta, h, V)$ by linear interpolation.

$Q^*(V_0)$ is found by performing a one-dimensional search over altitude for a given velocity V_0. A coarse grid is set up ranging from 0 to 80,000 ft with increments of 5000 ft. The fuel flow $Q(\eta, h, V_0)$ is evaluated at each altitude grid point (with fixed velocity V_0). The minimizing altitude (h_1) is then picked out by direct comparison of fuel-flow values. Another search is carried out over a range of 10,000 ft centered at altitude h_1, with a grid size of 500 ft. A refined estimate of the minimizing altitude (h_2) is obtained by comparing values of fuel flow. Finally, a golden-section search is performed over the 1000-ft interval centered at h_2, with an accuracy of 0.1 ft. It was observed from plots of $Q(\eta, h, V_0)$ vs h that $Q(\eta, h, V_0)$ satisfies the unimodality requirement near the minimum; hence the golden-section search is successful.

The minimizing altitude obtained from the golden-section is h_0 and the corresponding throttle setting is η_0. Thus, one finds that

$$Q^*(V_0) = \min_h [Q(\eta, h, V_0)] = Q(\eta_0, h_0, V_0)$$

In this manner, $Q^*(V)$ can be computed for any given velocity.

Acknowledgments

This research was supported by NASA Langley Research Center under Grant NAG 1-203. Dr. Christopher Gracey served as NASA Technical Officer.

References

[1]Kelley, H. J., "Aircraft Maneuver Optimization by Reduced-Order Approximation," *Control and Dynamic Systems,* Vol. 10, edited by C. T. Leondes, Academic Press, New York, pp. 131-178.

[2]Bryson, A. E. and Ho, Y. C., *Applied Optimal Control,* Hemisphere Publishing Co., Washington, 1969.

[3]Leitmann, G., *An Introduction to Optimal Control,* McGraw-Hill Book Co., New York, 1966.

[4]Luenberger, D. G., *Optimization by Vector Space Methods,* John Wiley & Sons, New York, 1969, pp. 131-133.

[5]Marchal, C., "Chattering Arcs and Chattering Controls," *Journal of Optimization Theory and Applications,* Vol. 11, 1973, pp. 441-468.

[6]Houlihan, S. C., Cliff, E. M., and Kelley, H. J., "A Study of Chattering Cruise," *Journal of Aircraft,* Vol. 19, Feb. 1982, pp. 119-124.

[7]Gilbert E. G. and Parsons, M. G., "Periodic Control and the Optimality of Aircraft Cruise," *Journal of Aircraft,* Vol. 13, Oct. 1976, pp. 828-830.

[8]Speyer, J. L., "Nonoptimality of the Steady-State Cruise for Aircraft," *AIAA Journal,* Vol. 14, Nov. 1976, pp. 1604-1610.

[9]Mummolo, F. and Lefton, L., "Cubic Splines and Cubic-Spline Lattices for Digital Computation," Analytical Mechanics Associates Inc., Rept. 72-28, July 1972, revision dated Dec. 1974.